

The same, but different: stochasticity in binary destruction

Richard J. Parker^{1★} and Simon P. Goodwin²

¹*Institute for Astronomy, ETH Zürich, Wolfgang-Pauli-Strasse 27, 8093 Zürich, Switzerland*

²*Department of Physics and Astronomy, University of Sheffield, Sheffield S3 7RH*

Accepted 2012 April 26. Received 2012 April 24; in original form 2012 February 7

ABSTRACT

Observations of binaries in clusters tend to be of visual binaries with separations of tens to hundreds of au. Such binaries are ‘intermediates’ and their destruction or survival depends on the exact details of their individual dynamical history. We investigate the stochasticity of the destruction of such binaries and the differences between the initial and processed populations using N -body simulations. We concentrate on Orion nebula cluster-like clusters, where the observed binary separation distribution ranges from 62 to 620 au.

We find that, starting from the same initial binary population in statistically identical clusters, the number of intermediate binaries that are destroyed after 1 Myr can vary by a factor of >2 , and that the resulting separation distributions can be statistically completely different in initially substructured clusters. We also find that the mass ratio distributions are altered (destroying more low mass-ratio systems), but not as significantly as the binary fractions or separation distributions. We conclude that finding very different intermediate (visual) binary populations in different clusters does not provide conclusive evidence that the initial populations were different.

Key words: methods: numerical – binaries: general – stars: formation – open clusters and associations: general.

1 INTRODUCTION

The nature of star formation is one of the great unsolved problems in astrophysics. The formation of stars is extremely interesting in itself, but also has implications for galaxy formation and evolution, and planet formation. In recent years, studies of young star-forming regions have shown that the initial mass function (IMF) is invariant, at least on nearby galactic scales (Bastian, Covey & Meyer 2010).

It is unclear whether this apparent universality of star formation in the IMF is also mirrored in the primordial binary population. Most stars form in binaries (Goodwin & Kroupa 2005; Kroupa 2008), but the picture is clouded by subsequent dynamical evolution in some clustered environments (e.g. Kroupa 1995a,b; Parker et al. 2009; Parker, Goodwin & Allison 2011), making it difficult to conclude whether or not binary formation in different star-forming regions is also universal (King et al. 2012).

By comparing the results of N -body simulations to observations of binaries in both clusters and the Galactic field, it is possible to account for this dynamical evolution and then infer the probable initial conditions of star formation, a process known as ‘reverse engineering’ or ‘inverse population synthesis’ (Kroupa 1995a). For this purpose the results of many simulations (≥ 10) are usually

averaged together to obtain a 1σ uncertainty, and are then compared to observations.

Most observations of the binary separation distribution in young clusters tend to probe the visual separation regime (e.g. Patience et al. 2002; Reipurth et al. 2007; King et al. 2012), in which binaries typically have separations between several tens and several hundreds of au (this depends on distance and cluster surface density).

Taking the Orion nebula cluster (ONC) as an example, the observations probe the separation range 62–620 au (Reipurth et al. 2007). Binaries with shorter separations are difficult to detect in clusters, whereas those with wider separations become indistinguishable against the background of other cluster members (even if they exist in such clusters; Scally, Clarke & McCaughrean 1999; Parker et al. 2009). Comparison with averaged numerical simulations (Parker et al. 2009, 2011) suggests good agreement with a primordial field-like separation distribution and an initial binary fraction of around 75 per cent.

Unfortunately, as we will investigate in detail in this paper, this tens to hundreds of au ‘intermediate’ binary separation range is one which is affected stochastically by dynamical interactions.

Heggie (1975) and Hills (1975) investigated the dynamical processing of binaries. They divided binaries into two broad classes: hard and soft. Hard binaries have a binding energy that exceeds the local Maxwellian energy of stars in the cluster and are so tightly bound that it is extremely rare for an encounter to destroy them

★E-mail: rparker@phys.ethz.ch

(indeed, encounters tend to extract energy, making them harder). Soft binaries have a binding energy that is less than the local Maxwellian energy and are so loosely bound that a single distant encounter, or even the tidal field of a cluster, can destroy them (although they are so easy to make that a transient population can exist, see Moeckel & Clarke 2011).

Based on these definitions, it is also possible to define a third dynamical class of binaries: intermediate binaries. Intermediate binaries are those in between hard and soft (their binding energy is comparable to the local Maxwellian energy of stars in the cluster), whereby a single relatively close encounter, or several distant encounters *may* destroy them. Therefore whether an intermediate binary survives depends on the exact details of its dynamical history and an element of ‘luck’ in the number and severity of encounters it has.

In a smooth, spherical system such as a Plummer sphere, the boundary between hard and soft binaries, a_{hs} , can be estimated following Binney & Tremaine (1987) as

$$a_{\text{hs}} = \frac{3}{2} \frac{r_{1/2}}{N_{\text{sys}}}, \quad (1)$$

where $r_{1/2}$ is the half-mass radius of the cluster and N_{sys} is the number of stellar systems in the cluster. Adopting the current half-mass radius of the ONC as 0.8 pc (Hillenbrand & Hartmann 1998), and the number of stars as ~ 1500 (King et al. 2012), then $a_{\text{hs}} \simeq 250$ au.

However, the hard–soft boundary is not a sharp boundary. Destruction depends not only on the typical encounter energy/velocity, but also on having an encounter, and hence an element of ‘luck’ in having or avoiding a destructive encounter. The encounter time-scale depends on density, but with (as we will show) a stochastic element.¹ Binaries a factor of 2 or 3 above a_{hs} can survive if they avoid strong encounters, and binaries a factor of 2 or 3 below a_{hs} can be destroyed.

As the hard–soft boundary depends on *local* density, it varies radially in smooth distributions such as Plummer spheres. It is also a very difficult quantity to define in substructured distributions such as fractals as the density can vary significantly.

In this paper, we investigate the consequences of the stochasticity of intermediate binary destruction in star clusters. This is particularly important because, as we have discussed, observations generally cover the intermediate binary population. We evolve a variety of clumpy and smooth clusters containing exactly the same initial binary population (identical primary and secondary masses, semimajor axes and eccentricities) and examine the intermediate binary population after 1 Myr. We describe the simulation set-up in Section 2, present our results in Section 3, provide a discussion in Section 4 and conclude in Section 5.

2 METHOD

In this section, we describe the method used to set up and run the numerical simulations of our model clusters.

¹ In the Galactic field, the hard–soft boundary is formally much lower than that in clusters as the velocity dispersion is much higher than that in clusters. However, many formally soft binaries can survive for Gyr as the encounter time-scale is so long.

2.1 Binary population

We set up the clusters with only one primordial binary population. This enables an investigation into the effects of morphology and dynamics on a constant initial separation distribution of intermediate binaries to compare to the observational data.

Earlier work has shown that in a dense ONC-like cluster, a primordial binary population will be affected by dynamical interactions, which both lowers the primordial binary fraction and alters the initial semimajor axis (hereafter separation) distribution (e.g. Kroupa, Petr & McCaughrean 1999; Parker et al. 2009, 2011).

Recently, King et al. (2012) have placed observational and theoretical constraints on the primordial binary fraction and separation distribution in the ONC, and found that a G-dwarf field-like separation distribution (Duquennoy & Mayor 1991; Raghavan et al. 2010) and an initial binary fraction of ~ 75 per cent (also confirmed from theoretical considerations by Kaczmarek, Olczak & Pfalzner 2011; Parker et al. 2011) represent the most likely primordial binary population.

In this work, we adopt an initial binary fraction of 100 per cent and a field-like separation distribution (Duquennoy & Mayor 1991; Fischer & Marcy 1992; Raghavan et al. 2010). As our clusters are relatively dense initially, the widest binaries in the field-like separation distribution are not physically bound (Parker et al. 2009), and the starting binary fraction in the simulations is closer to 75 per cent.

We draw the primary masses from a Kroupa (2002) IMF of the form

$$N(M) \propto \begin{cases} M^{-1.3} & m_0 < M/M_{\odot} \leq m_1, \\ M^{-2.3} & m_1 < M/M_{\odot} \leq m_2, \end{cases} \quad (2)$$

where $m_0 = 0.1$, $m_1 = 0.5$ and $m_2 = 50 M_{\odot}$. We do not include brown dwarfs in the simulations as these are not present in the observational samples with which we will compare our simulations. Secondary masses are drawn from a flat mass ratio distribution, in accordance with observations of the distribution in the Galactic field (Reggiani & Meyer 2011). However, we limit the lower mass of a companion to be $0.1 M_{\odot}$; this means that lower mass stars do not have a full range of mass ratios. For example, a $0.15 M_{\odot}$ primary can only have companions in the range 0.1 – $0.15 M_{\odot}$. If a companion of mass $< 0.1 M_{\odot}$ is selected, we draw a new random mass ratio until a companion $\geq 0.1 M_{\odot}$ is selected.

In accordance with observations of the field, we select binary periods from the log-normal fit to the G-dwarfs in the field by Duquennoy & Mayor (1991) – see also Raghavan et al. (2010), which has also been extrapolated to fit the period distributions of the K- and M-dwarfs (Fischer & Marcy 1992; Mayor et al. 1992):

$$f(\log_{10} P) \propto \exp \left\{ -\frac{(\log_{10} P - \overline{\log_{10} P})^2}{2\sigma_{\log_{10} P}^2} \right\}, \quad (3)$$

where $\overline{\log_{10} P} = 4.8$, $\sigma_{\log_{10} P} = 2.3$ and P is in days. We convert the periods to semimajor axes using the masses of the binary components.

The eccentricities of binary stars are drawn from a thermal distribution (Heggie 1975; Kroupa 2008) of the form

$$f_e(e) = 2e. \quad (4)$$

In the sample of Duquennoy & Mayor (1991), close binaries (with periods less than 10 d) are almost exclusively on tidally circularized orbits. We account for this by reselecting the eccentricity of a system

if it exceeds the following period-dependent value:

$$e_{\text{tid}} = \frac{1}{2} [0.95 + \tanh(0.6 \log_{10} P - 1.7)]. \quad (5)$$

We combine the primary and secondary masses of the binaries with their semimajor axes and eccentricities to determine the relative velocity and radial components of the stars in each system. The binaries are then placed at the centre of mass and velocity for each system in either the fractal distribution or Plummer sphere (see Section 2.2).

Note that the exact details of the initial binary distribution do not matter. The following results would be true of *any* initial distribution of intermediate binaries in a cluster.

2.2 Cluster morphologies

We set up clusters containing 1500 stars (i.e. 750 binary systems) and adopt two different morphologies. First, we create fractal clusters (Cartwright & Whitworth 2004; Goodwin & Whitworth 2004) to create clusters with substructure, and secondly, we use Plummer spheres (Plummer 1911) to enable a comparison between centrally concentrated, smooth clusters and the substructured clusters.

2.2.1 Fractal clusters

Observations of young, dynamically unevolved star-forming regions indicate that a large amount of substructure is present (e.g. Cartwright & Whitworth 2004; Sánchez & Alfaro 2009). The most convenient way of describing substructure is via the fractal, in which the amount of substructure is set by just one number, the fractal dimension, D (Goodwin & Whitworth 2004). We adopt a moderate amount of substructure ($D = 2.0$).

The velocities of systems in the fractal are drawn from a Gaussian of mean zero, and the fractal is constructed in such a way that nearby stars have similar velocities, whereas the velocities of distant stars can be very different (see Goodwin & Whitworth 2004; Parker et al. 2011, for a more detailed description). The initial radius of the fractal is 1 pc, and we scale the velocities so the cluster has a virial ratio $Q = 0.3$, which is subvirial or ‘cool’. These initial conditions have been successful in explaining the level of mass segregation in the ONC through dynamics (Allison et al. 2009, 2010) and can account for the formation of trapezium-like systems (Allison & Goodwin 2011).

2.2.2 Plummer spheres

No two fractals are identical and to the eye two statistically identical fractals can look very different. It is therefore desirable to test whether any differences in the intermediate separation distribution are not simply due to the exact details of the fractal realizations. We therefore conduct simulations in which we evolve the same primordial binary population in a radially smooth, centrally concentrated Plummer sphere (Plummer 1911). Whilst no two Plummer spheres are identical, their initial structures and their evolution are much more similar than fractals.

The positions and velocities of the systems are determined according to the prescription in Aarseth, Hénon & Wielen (1974). We construct Plummer spheres with an initial half-mass radius $r_{1/2} = 0.1$ pc (corresponding to a hard–soft boundary of ~ 70 au) and set them to be in virial equilibrium initially ($Q = 0.5$).

The binaries are then randomly assigned a system position and velocity in the fractal or Plummer sphere, which vary with each

realization of the cluster morphology. We run 10 realizations of each morphology, identical apart from the random number seed used to initialize the positions and velocities of the systems. In each cluster, we place the same population of binary stars (see Section 2.1). We do not include stellar evolution in the simulations. The simulations are run for 1 Myr using the *kira* integrator in the *STARLAB* package (e.g. Portegies Zwart et al. 1999, 2001).

2.3 Summary

To summarize, we take a single initial binary population, always the same in every way, and place it in 10 realizations of a fractal cluster and 10 realizations of a Plummer sphere. We evolve each cluster for 1 Myr and examine the remaining intermediate binary population in each cluster.

We have chosen to compare our simulations with the ONC. First, there are good observations of visual binaries in the ONC in the separation range 62–620 au (Reipurth et al. 2007). Secondly, the density of the ONC suggests that the hard–soft boundary lies within this separation range (Kroupa et al. 1999; Parker et al. 2009).² Finally, the ONC has a large enough population ($N \sim 1500$ stars) that we have a significant population in this separation range in each cluster. In later papers, we will discuss other separation ranges, different cluster masses and the effects of small number statistics, but for now we will concentrate on the currently observed intermediate binary population in a fairly massive ONC-like cluster.

3 RESULTS

Our *initial* binary population is formed with 106 binaries in the range 62–620 au, and this is the initial population for *every* cluster. Clusters differ only in the random number seeds which set the system positions and velocities, not the system properties.

In this section, we will first examine the differences in the numbers of intermediate binaries which are destroyed after 1 Myr, before turning our attention to the separation distributions and the mass ratio distributions of these binaries.

3.1 Binary fraction

In Table 1, we present the initial (0 Myr) and final (1 Myr) numbers of binaries in the separation range 62–620 au in each of the 10 fractal cluster simulations. Each cluster has 106 binaries in this range initially, but the final number of binaries varies significantly, with extrema of 62 and 87 binaries (simulations i and a, respectively). Thus between 42 and 18 per cent of the initial population has been destroyed. Looking just at this range, we started with 212 stars in 106 systems (a binary fraction of unity³) and the extremes after 1 Myr are 212 stars in 150 systems (a binary fraction of 0.41) and 212 stars in 125 systems (a binary fraction of 0.70).

Turning to the Plummer-sphere clusters, in Table 2 we show the initial (0 Myr) and final (1 Myr) numbers of binaries in the separation range 62–620 au for each of our 10 simulated clusters.

² In this paper, we will keep the separation range fixed with which we compare the simulations, but we note that our two different suites of simulations may have quite different hard–soft boundaries. For example, our Plummer-sphere clusters reach higher densities (and therefore contain more soft binaries) than the fractal clusters.

³ We define the binary fraction, $f_{\text{bin}} = \frac{B}{S+B}$, where B is the number of binaries (and higher order multiple systems) and S is the number of singles.

Table 1. The numbers of binaries in the separation range 62–620 au in the fractal cluster simulations at 0 Myr (first row) and at 1 Myr (second row). Each simulation has 106 binaries initially.

Simulation	a	b	c	d	e	f	g	h	i	j
$N_{\text{bin};0 \text{ Myr}}$	106	106	106	106	106	106	106	106	106	106
$N_{\text{bin};1 \text{ Myr}}$	87	83	67	74	73	77	66	81	62	69

Table 2. The numbers of binaries in the separation range 62–620 au in the Plummer-sphere cluster simulations at 0 Myr (first row) and at 1 Myr (second row). Not all 106 binaries are physically bound at the start of each simulation due to the high initial densities of the Plummer spheres.

Simulation	a	b	c	d	e	f	g	h	i	j
$N_{\text{bin};0 \text{ Myr}}$	102	100	102	103	105	104	104	101	104	102
$N_{\text{bin};1 \text{ Myr}}$	48	39	61	42	54	65	52	50	64	54

There is a slight variation in the initial number of binaries detected by our algorithm (and no cluster has its full complement of 106 initial binaries identified), due to the high initial densities of the Plummer spheres.

In the two most extreme cases, 39 binaries remain in a cluster that contained 100 initially (simulation b) and 65 binaries remain in a cluster that contained 105 initially (simulation f). Thus, between 71 and 37 per cent of the initial population has been destroyed. In terms of the binary fraction, we started with 212 stars in 112 systems (a binary fraction of 0.89 – simulation b), and 212 stars in 108 systems (a binary fraction of 0.96 – simulation f). After 1 Myr the binary fractions in these clusters are 0.23 and 0.44, respectively.

The *total* binary fraction in the cluster, of course, also depends on the numbers of systems with separations outside of this range that have been destroyed.

More binaries are destroyed in the Plummer-sphere clusters than the fractal clusters. The reason for this is that we produce an intermediate binary (say of separation 500 au) and place it at random within the simulation. If the binary is placed in a low-density region where the typical separation between stars is, say, 3000 au, then it is clearly identified as a binary system. However, if a 500 au binary is placed in a dense region with a typical inter-star separation of, say, 800 au, then it is no longer a ‘binary’. The handful of 106 intermediate separation systems placed near the centre of a Plummer sphere are therefore ‘destroyed’ at time zero.

The localized substructure in the fractal clusters is not as dense as the central regions of the Plummer spheres, and so all binaries that ‘form’ in the fractals remain physically bound. The maximum densities in the fractal clusters are around $1000\text{--}2000 \text{ M}_{\odot} \text{ pc}^{-3}$, whilst the central densities of the Plummer spheres are around $6\text{--}7 \times 10^4 \text{ M}_{\odot} \text{ pc}^{-3}$. Therefore, as the simulation progresses there will be significantly more and closer encounters in the centres of the Plummer spheres, which process the intermediate binaries more than in fractal clusters. We noted above that after 1 Myr, the 106 intermediate binaries in the fractal clusters had been reduced to between 62 and 87 systems. In the much denser Plummer spheres, the final numbers of systems are between 39 and 65 – a far more destructive environment.

However, in both morphologies the final binary fractions can differ by almost a factor of 2, irrespective of density.

3.2 Separation distribution

As well as changing the binary fraction in the intermediate range 62–620 au, the distribution of separations can also be changed significantly.

In Fig. 1, we show the individual separation distributions in the range 62–620 au for each fractal cluster binned in the same way as the data in Reipurth et al. (2007). The initial separation distribution, which is identical in each simulation, is shown by the open histogram, and the separation distribution after 1 Myr is shown by the shaded histogram. For comparison, the data from Reipurth et al. (2007) are shown by the green crosses, and the log-normal fits to the field separation distributions for the G- and M-dwarfs are shown by the solid red and dashed blue lines, respectively. The average of all 10 simulations, with 1σ uncertainties, is shown in panel (k).

As noted in Parker et al. (2011), averaging together the 10 realizations of clusters with a fractal morphology and subvirial velocities reproduces the observed ONC binary distribution reasonably well (see also King et al. 2012). However, from the inspection of Fig. 1 we see that the same initial population can evolve to very different distributions over the course of 1 Myr. Clearly, the initial population of 106 intermediate binaries is processed differently in each cluster.

In Fig. 2, we show the cumulative distributions of the intermediate binary separations along with the initial separation distribution (the thick dashed grey line in both panels). In Fig. 2(a), all 10 fractal realizations are shown; in Fig. 2(b) we show the two most different cumulative distributions.

In Fig. 3, we plot the 45 possible Kolmogorov-Smirnov (KS)-test comparisons between the cumulative separation distributions of the fractal clusters. We reject the null hypothesis of there being no difference between two separation distributions if the KS p -value is less than 0.05.

The two most different separation distributions are from the distributions shown in panels (c) and (h) of Fig. 1. Note that these two simulations are not the same two simulations that produce the largest difference in binary fraction (which were those in panels a and i).

The largest difference between the two extreme distributions is $D = 0.26$; for this D a KS test gives the p -value $\mathcal{P} = 0.01$. This is a very significant difference and one would draw the (correct)

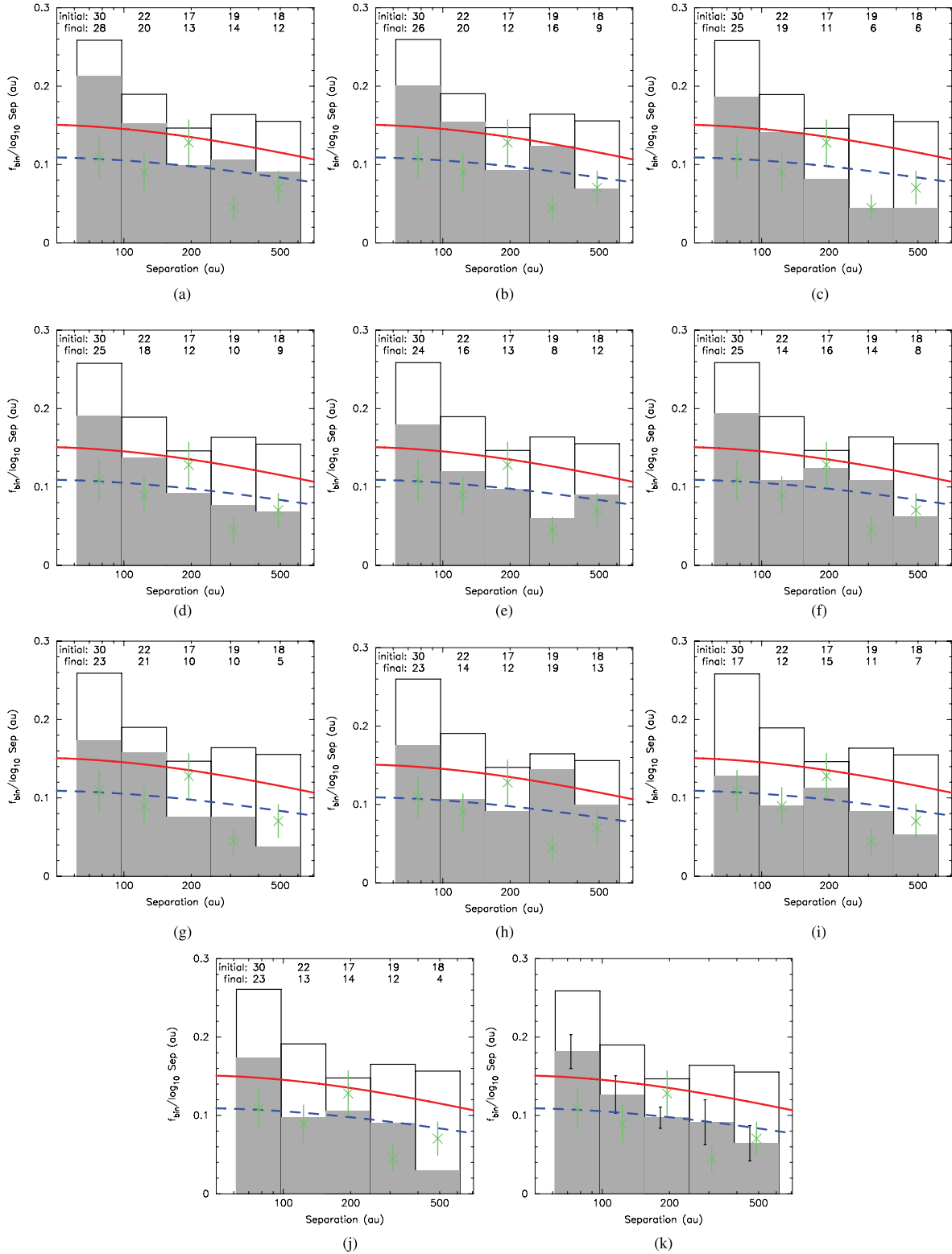


Figure 1. Individual intermediate separation distributions in the range (62–620 au) probed by Reipurth et al. (2007) (panels a–j). The average of all 10 simulations is shown in panel (k). The (constant) initial distribution is shown by the open histogram, and the final distribution is shown by the shaded histogram. The observations by Reipurth et al. (2007) are shown by the green crosses. The log-normal fits to the field separation distributions for the G- and M-dwarfs are shown by the solid red and dashed blue lines, respectively. Along the top are the initial and final numbers of binaries in each bin; note that the initial numbers of binaries are always the same.

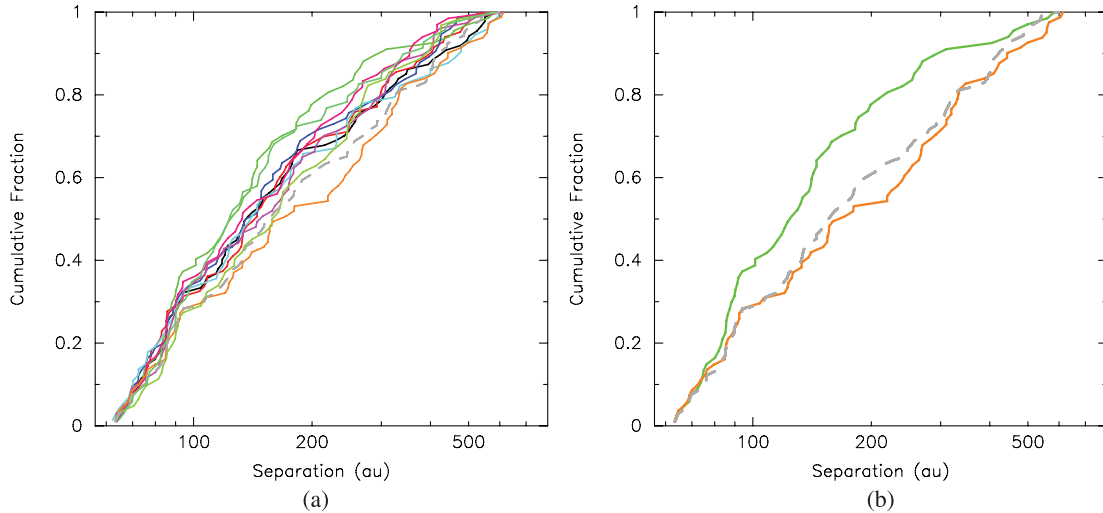


Figure 2. The cumulative separation distribution of binaries in the separation range 62–620 au in (a) 10 different fractal clusters and (b) the two extrema, after 1 Myr. The initial binary population is shown by the thick dashed grey line in both panels and is identical for each cluster.

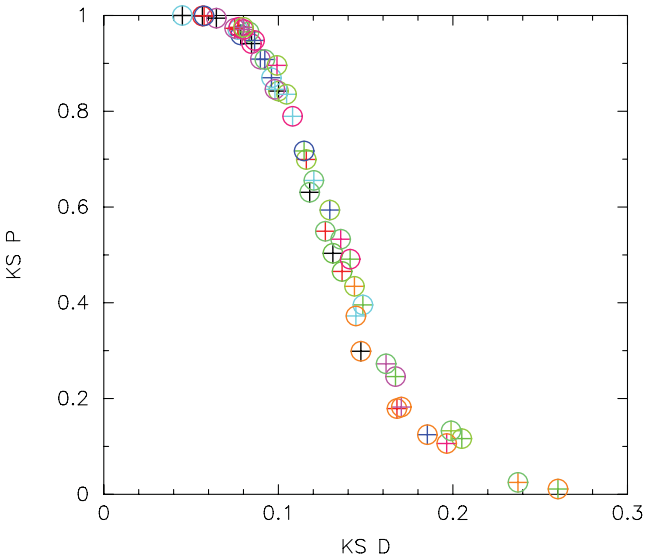


Figure 3. The distribution of values for KS tests between all pairs of the fractal cluster simulations on the cumulative separation distributions (colours correspond to those in Fig. 2). We show the KS p -value against the KS \mathcal{D} statistic.

conclusion that these two distributions are different. However, it is not the *initial* distributions that were different (they were identical); rather it is the dynamical processing of the systems that was very different.

Note that only two pairs of simulations are rejected by the KS test as being significantly different (pairs c and h, and h and j), with simulation h being the most significant outlier. That nine simulations agree reasonably well with each other (for the separation distribution, not necessarily, as we have seen for binary fractions) shows that this simulation is just an outlier. However, the problem is that in just 10 simulations we have produced a significant outlier, and there is no way of telling if a single observed distribution for a cluster is such an outlier.

Examination of Fig. 2(b) shows that one extreme (the lower orange line) remains very close to the initial separation distribution (the thick dashed grey line). This distribution is from panel (h) of Fig. 1, and it can be seen that it has lost roughly the same fraction of binaries from each bin so retaining the shape of the initial distribution. The upper extreme (the green line) shows a very different separation distribution to the initial distribution, as can also be seen in panel (c) of Fig. 1 this cluster has mainly lost wider binaries (>200 au).

Generally speaking (and visible in Figs 1 and 2), wider binaries are more susceptible to disruption as they are more weakly bound. A key result, however, is that because binary destruction is stochastic, the probability of destruction of an *intermediate* system depends more on whether a system has had a close encounter or not than on the binding energy of the system (see Heggie 1975; Hills 1975).

One could hypothesize that the very different and stochastic dynamical histories of different fractals (see Allison et al. 2010) might be responsible for the very large differences in the resulting populations. To test this, in Fig. 4 we plot the cumulative distributions of separations in our 10 Plummer spheres for all 10 realizations (panel a) and the two extremes (panel b) after 1 Myr along with the initial distribution (the thick dashed grey lines). Note that the initial distributions for each Plummer sphere are very slightly different; this is because some intermediate systems are in such a place that they are not identified as binaries even at time zero. Different realizations of Plummer spheres are almost impossible to distinguish, and their dynamical histories will be very similar. The only differences should be in the chance of a particular system having (a) destructive encounter(s) or not.

Again we find a wide spread in the distributions, and we plot the results of the KS tests between each set of simulations in Fig. 5. Interestingly, although the Plummer spheres are more dense, the most extreme separation distributions (shown in Fig. 4b) have $\mathcal{D} = 0.23$ and a KS test p -value $\mathcal{P} = 0.15$. Based on this value, we cannot reject the hypothesis that there is no difference between these separation distributions. However, as we have seen, the binary fractions are also significantly affected, and care must be taken not to take a marginal result for the KS test in the separation distribution together with different binary fractions to make us suspect a real difference between clusters.

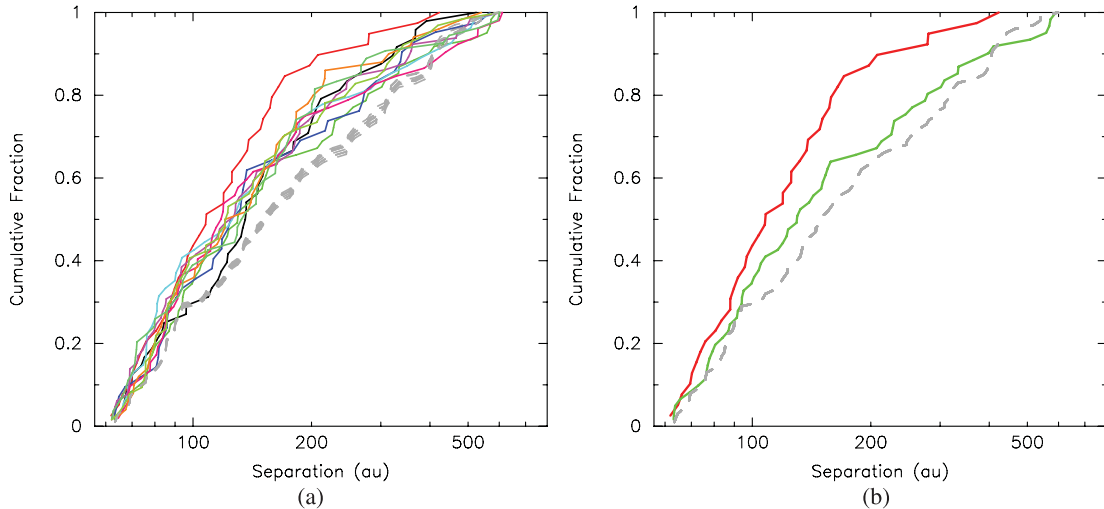


Figure 4. The cumulative separation distribution of binaries in the separation range 62–620 au in (a) 10 different Plummer-sphere clusters and (b) the two extrema, after 1 Myr. In panel (a) the thick dashed grey lines show the initial distributions which are slightly different for each cluster (see the text); the differences are so small that in panel (b) we only plot the primordial distribution for the right-hand cluster for clarity.

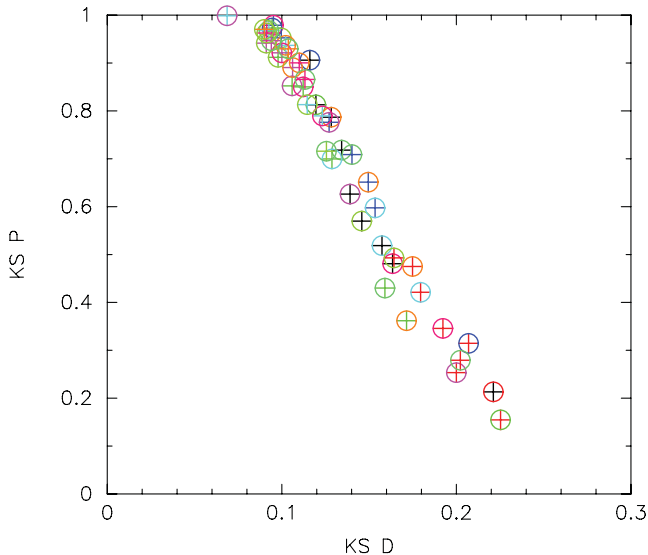


Figure 5. The distribution of values for KS tests between all pairs of the Plummer-sphere cluster simulations on the cumulative separation distributions (colours correspond to those in Fig. 4). We show the KS p -value against the KS \mathcal{D} statistic.

This may indicate that the differences in the final separation distributions are due to the stochastic nature of the substructured fractals. However, as young, unevolved clusters appear to be substructured (Cartwright & Whitworth 2004; Sánchez & Alfaro 2009), and this substructure can disrupt binaries (Parker et al. 2011; King et al. 2012), we must recognize that this stochasticity could affect our interpretation of observations of real clusters.

3.3 Mass ratio distribution

We have seen that the numbers and separation distributions of intermediate binaries can be significantly altered in a highly stochastic way by encounters. We now turn our attention to the mass ratio distribution: is this also significantly altered or does it retain an

imprint of the initial distribution? Note that the initial mass ratio distribution for our binary population is flat.⁴

In Figs 6 and 7, we show the cumulative distributions of mass ratios in the intermediate range 62–620 au after 1 Myr of the fractal clusters (Fig. 6) and the Plummer spheres (Fig. 7). In both figures, panel (a) shows all 10 realizations and panel (b) shows the two most extreme distributions. The initial mass ratio distributions are shown by the thick dashed grey lines (for the same reasons as in the separation distributions, each Plummer sphere has a *slightly* different initial distribution).

Interestingly in the fractal clusters, the spread in the mass ratio distributions is rather low (Fig. 6), and even the two extremes look very similar (panel b). A KS test on these distributions fails to distinguish them.

However, in the Plummer spheres where processing has been much more extreme, we see that the difference between the two extremes is greater than in the fractal clusters, but still not enough to be significantly different in a KS test.

Finally, we note that both the fractals and Plummer spheres with the two extremes in the final mass ratio distribution are *not* the same clusters with the extremes in the separation distribution.

Whether an encounter is destructive depends on the distance of that encounter and the binding energy of the binary: a closer binary requires a closer encounter to destroy it. Binding energy also depends on the mass ratio, but these results suggest that the most important factor is the distance of the encounter (which depends on density but is stochastic with regard to the mass ratio of the system). In the case of the Plummer-sphere clusters (Fig. 7b) both clusters have *more* $q < 0.4$ systems after processing than before (inspection of Fig. 7a shows that this is not always the case). One extreme has stayed fairly close to the initial mass ratio distribution (the upper extreme), whilst the lower extreme has evolved to have far more very high mass ratio systems ($q > 0.9$).

⁴ The cumulative initial mass ratio distributions in Figs 6 and 7 are not straight lines despite being drawn from a flat mass ratio distribution. This is due to limiting the lower mass of companions to be $> 0.1 M_{\odot}$, meaning that the M-dwarfs in particular do not fill the entire range of possible mass ratios. See Section 2.

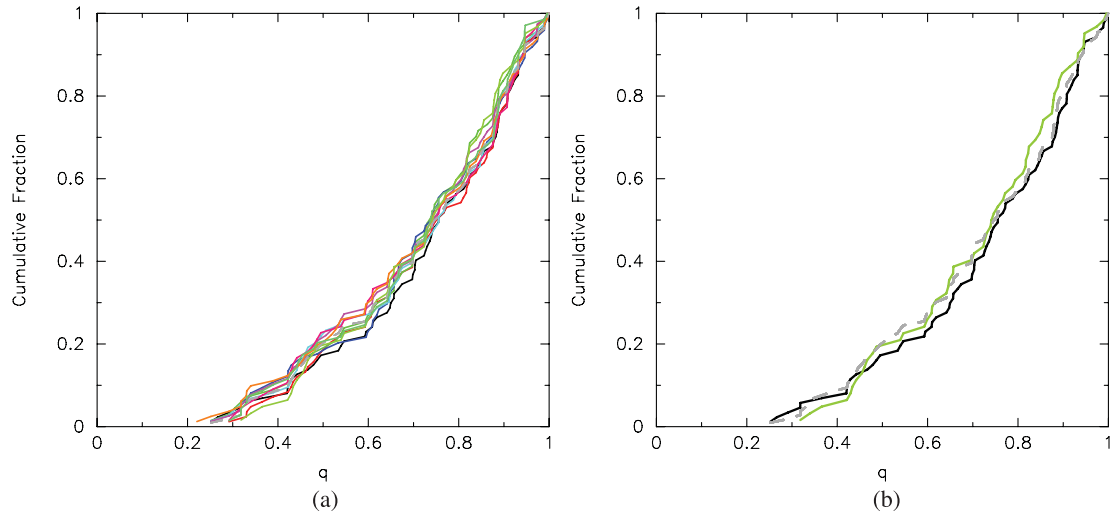


Figure 6. The cumulative mass ratio distribution of binaries in the separation range 62–620 au in (a) 10 different fractal clusters and (b) the two extrema, after 1 Myr. The initial distribution is shown by the thick dashed grey line in both panels.

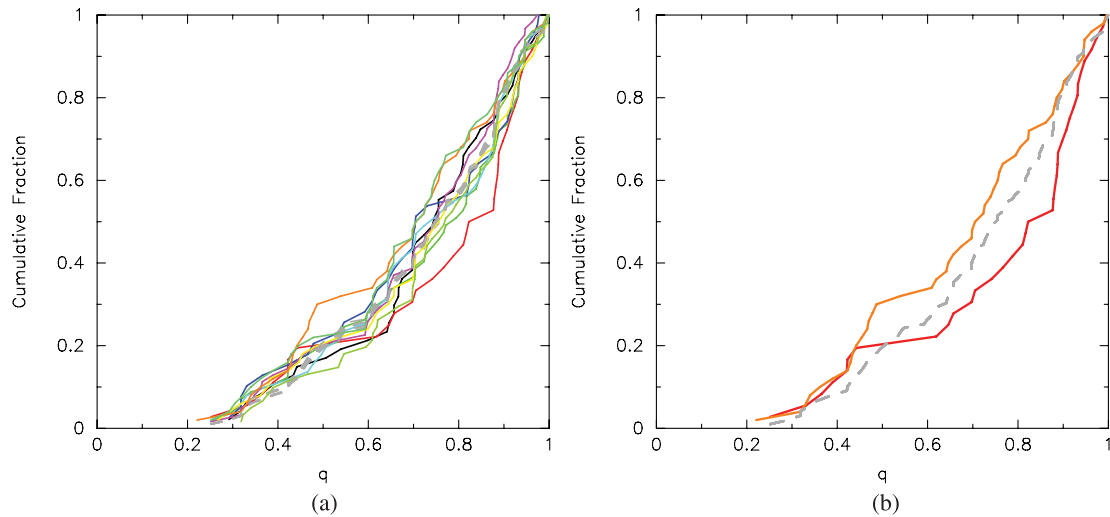


Figure 7. The cumulative mass ratio distribution of binaries in the separation range 62–620 au in (a) 10 different Plummer-sphere clusters and (b) the two extrema, after 1 Myr. The initial distributions are shown by the thick dashed grey line in panel (a), but in panel (b) the initial distribution for the right-hand cluster only is shown for clarity.

4 DISCUSSION

From the results presented in Section 3 we can see that stochasticity in the destruction of intermediate binaries can have a number of important consequences.

As would be expected, intermediate binary destruction depends on density. Dense environments are far more effective at destroying intermediate binaries. Indeed, the definition of what is a hard, soft or intermediate binary depends on density – a hard binary in a very low density environment could be an intermediate binary in another environment.

However, the range of (visual) binary separations in clusters normally probed by observations (tens to hundreds of au) covers the intermediate binary regime in the range of densities found in those clusters ($10\text{--}10^5\text{ stars pc}^{-3}$) (see King et al. 2012). Therefore, we almost always observe intermediate binaries in star-forming regions.

As would be expected, we find that the number of binaries processed depends on density. But this processing is always stochastic

with 18–42 per cent of intermediate binaries processed in the relatively low-density fractals to 37–71 per cent in the higher density Plummer spheres. Therefore, the number of intermediate binaries that are destroyed depends on density, but with a stochastic factor of around 2 in the number destroyed.

A key result is illustrated in Figs 2 and 4 that whatever the density, the initial intermediate separation distribution can be significantly altered. Wider intermediate binaries are generally destroyed in preference to closer intermediates, but this is not a strong relationship. For an initially substructured cluster, differences in processing can easily be extreme enough to show very strong statistical differences with, e.g., a KS test. We emphasize here that only two different pairs of simulations resulted in significantly different separation distributions. However, we have no way of telling whether the clusters we observe in reality are themselves stochastic outliers.

Interestingly, as shown in Figs 6 and 7, the change in the initial mass ratio distributions is not as strong as in the separation distributions. It seems that intermediate binary destruction does not

care about the system's mass ratio. That intermediate binary destruction is insensitive to mass ratio means that the processed mass ratio distributions are statistically the same as the initial mass ratio distribution. Therefore, in clusters with low levels of intermediate binary destruction, the mass ratio distribution should reflect the initial mass ratio distribution. However, one has to know that there has been little processing to use this result.

These results have interesting implications for the interpretation of both observations and numerical simulations.

Clearly, when we observe a cluster we are observing a single realization of its initial binary population and the processing of that population. When we compare two clusters we are comparing two different realizations, and as we have seen, any two realizations may be very different, even if their initial conditions were the same.

Further, as we have seen, the dynamical processing of intermediate binaries does depend on density. It is important to note that processing occurs very quickly and so it is not the current density that is important, but the maximum density reached at some point in the past that determines how effective binary processing is (see also Parker et al. 2009, 2011; Goodwin 2010).

The problem we face when attempting to compare two intermediate binary populations and to determine if they come from the same initial populations is therefore twofold. First, we need to have information about the past state of the cluster to determine what level of processing we might expect *on average*. Secondly, we have to account for the stochasticity in intermediate binary destruction.

Let us take two ONC-like clusters as an example. We started with 106 binaries in the observed range 62–620 au. (Actually, random sampling from the same underlying distribution would give a range of 90–110 binaries initially in that range.) We then find that 37–71 per cent of these can be destroyed in a dense cluster. Therefore, in numbers of binaries alone, statistically the same initial population could result in between 39 and 65 binaries remaining in that range – a difference of over a factor of 2 from random chance alone. And this is before we consider the possibility that these two populations have also evolved to statistically different separation and mass ratio distributions.

If we were to observe two clusters with similar masses and densities, and find that they had statistically very significant differences in the numbers of binaries, and the separations and mass ratios of these binaries, then we might reasonably conclude that we were looking at two different initial populations and therefore a difference in how the stars were formed. However, as we have seen, that is sadly not the case.

Great care must also be taken when comparing simulations with observations. It is a standard procedure to average together the outcome of, say, 10 simulations and compare the separation distribution (with standard deviation) to the observed one (e.g. Kroupa et al. 1999; Parker et al. 2009, 2011; King et al. 2012). However, the observed distribution may in fact be an outlier, and a failure to fit the observed distribution might not mean that the model is ‘wrong’; conversely, a good fit to the observed distribution does not mean that the model is ‘right’ (correctly fitting an outlier would be worrying unless one’s simulation was also an outlier in the same way). The ensembles of simulations are crucial to at least determine a reasonable tolerance for the model; however, nothing will ever be able to determine whether the observed realization is an outlier or not.

In future papers, we will examine the observed binary separation distributions in clusters from King et al. (2012) in light of these results, and we will also examine which separation ranges are of

use in distinguishing differences or otherwise in the star formation in different regions.

5 CONCLUSIONS

We have conducted *N*-body simulations of ONC-like clusters containing 1500 stars (750 primordial binary systems) in which we have kept the initial binary population constant, but varied the positions and velocities of the systems within 10 realizations of the same cluster. We have studied two different cluster morphologies: a fractal cluster undergoing cool collapse (e.g. Allison et al. 2010) and a Plummer sphere in virial equilibrium (e.g. Parker et al. 2009). We have compared the intermediate separation distribution (62–620 au) in these clusters to examine the importance of stochasticity in intermediate binary destruction.

We conclude the following.

- (i) The numbers of intermediate systems destroyed in clusters can vary by a factor of 2.
- (ii) The separation distributions of intermediate systems in substructured clusters can be altered such that they are statistically significantly different after just 1 Myr.
- (iii) The mass ratio distributions change less than the separation distributions, especially in low-density environments.

The results imply that the intermediate binary separation distribution, which is the range most often observed in young clusters, should be treated with caution when used to interpret the dynamical history of a star cluster. Even with the knowledge of the initial conditions and the probable dynamical history of a cluster, stochasticity in intermediate binary destruction can very significantly alter the initial population. Whilst most clusters evolve in a ‘typical’ way, statistically significant outliers are not uncommon and we have no way of knowing if a single observed cluster is unusual because of differences in the initial conditions or through a slightly unusual dynamical evolution.

ACKNOWLEDGMENTS

We thank the anonymous referee for a prompt and helpful review. The simulations in this work were performed on the BRUTUS computing cluster at ETH Zürich.

REFERENCES

- Aarseth S. J., Hénon M., Wielen R., 1974, *A&A*, 37, 183
- Allison R. J., Goodwin S. P., 2011, *MNRAS*, 415, 1967
- Allison R. J., Goodwin S. P., Parker R. J., de Grijs R., Portegies Zwart S. F., Kouwenhoven M. B. N., 2009, *ApJ*, 700, L99
- Allison R. J., Goodwin S. P., Parker R. J., Portegies Zwart S. F., de Grijs R., 2010, *MNRAS*, 407, 1098
- Bastian N., Covey K. R., Meyer M. R., 2010, *ARA&A*, 48, 339
- Binney J., Tremaine S., 1987, *Galactic Dynamics*. Princeton Univ. Press, Princeton, NJ, p. 747
- Cartwright A., Whitworth A. P., 2004, *MNRAS*, 348, 589
- Duquennoy A., Mayor M., 1991, *A&A*, 248, 485
- Fischer D. A., Marcy G. W., 1992, *ApJ*, 396, 178
- Goodwin S. P., 2010, *R. Soc. Lond. Philos. Trans. A*, 368, 851
- Goodwin S. P., Kroupa P., 2005, *A&A*, 439, 565
- Goodwin S. P., Whitworth A. P., 2004, *A&A*, 413, 929
- Heggie D. C., 1975, *MNRAS*, 173, 729
- Hillenbrand L. A., Hartmann L. W., 1998, *ApJ*, 492, 540
- Hills J. G., 1975, *AJ*, 80, 809
- Kaczmarek T., Olczak C., Pfalzner S., 2011, *A&A*, 528, 144

- King R. R., Parker R. J., Patience J., Goodwin S. P., 2012, *MNRAS*, 421, 2025
- Kroupa P., 1995a, *MNRAS*, 277, 1491
- Kroupa P., 1995b, *MNRAS*, 277, 1507
- Kroupa P., 2002, *Sci*, 295, 82
- Kroupa P., 2008, in Aarseth S. J., Tout C. A., Mardling R. A., eds, *Lecture Notes in Physics*, Vol. 760, *Initial Conditions for Star Clusters*. Springer-Verlag, Berlin, p. 181
- Kroupa P., Petr M. G., McCaughrean M. J., 1999, *New Astron.*, 4, 495
- Mayor M., Duquennoy A., Halbwachs J.-L., Mermilliod J.-C., 1992, in McAlister H. A., Hartkopf W. I., eds, *ASP Conf. Ser. Vol. 32, IAU Colloq. 135: Complementary Approaches to Double and Multiple Star Research*. Astron. Soc. Pac., San Francisco, p. 73
- Moeckel N., Clarke C. J., 2011, *MNRAS*, 415, 1179
- Parker R. J., Goodwin S. P., Kroupa P., Kouwenhoven M. B. N., 2009, *MNRAS*, 397, 1577
- Parker R. J., Goodwin S. P., Allison R. J., 2011, *MNRAS*, 418, 2565
- Patience J., Ghez A. M., Reid I. N., Matthews K., 2002, *AJ*, 123, 1570
- Plummer H. C., 1911, *MNRAS*, 71, 460
- Portegies Zwart S. F., Makino J., McMillan S. L. W., Hut P., 1999, *A&A*, 348, 117
- Portegies Zwart S. F., McMillan S. L. W., Hut P., Makino J., 2001, *MNRAS*, 321, 199
- Raghavan D. et al., 2010, *ApJS*, 190, 1
- Reggiani M. M., Meyer M. R., 2011, *ApJ*, 738, 60
- Reipurth B., Guimarães M. M., Connelley M. S., Bally J., 2007, *AJ*, 134, 2272
- Sánchez N., Alfaro E. J., 2009, *ApJ*, 696, 2086
- Sclally A., Clarke C., McCaughrean M. J., 1999, *MNRAS*, 306, 253

This paper has been typeset from a \LaTeX file prepared by the author.